Available online at www.sciencedirect.com
SCIENCE DIRECT®
International Journal of Heat and Mass Transfer 48 (2005) 2186–2197
International Journal of HEAT and MASS TRANSFER
www.elsevier.com/locate/ijhmt

Condensation flow patterns in silicon microchannels

H.Y. Wu, P. Cheng *

School of Mechanical and Power Engineering, Shanghai Jiaotong University, Shanghai 200030, P.R. China

Received 6 June 2004; received in revised form 31 December 2004
Available online 5 March 2005

Abstract

A simultaneous visualization and measurement experiment was carried out to investigate condensation flow patterns of steam flowing through an array of trapezoidal silicon microchannels, having a hydraulic diameter of 82.8 μm and a length of 30 mm. The degassed and deionized water steam flowing in the microchannels was cooled by flowing water of 8 °C from the bottom. The silicon microchannels were covered with a thin transparent pyrex glass from the top which enabled the visualization of flow patterns. Experiments were performed at different inlet pressures ranging from 4.15×10^5 Pa to 1.25×10^5 Pa (with corresponding mass fluxes decreasing from 47.5 g/cm^2 s to 19.3 g/cm^2 s) while the outlet pressure was maintained at a value of 10^5 Pa. Different condensation flow patterns such as fully droplet flow, droplet/annular/injection/slug-bubbly flow, annular/injection/slug-bubbly flow, and fully slug-bubbly flow were observed in the microchannels. At a given inlet pressure and mass flux, the flow pattern depended on both the location and time. Of particular interest is that the vapor injection flow, consisting of a series of bubble growth and detachment activities, appeared and disappeared periodically. During the disappearance period of injection flow, the slug-bubbly flow at downstream changed to the single-phase liquid flow due to the reversed flow of outlet condensate, while the annular flow at upstream changed to the vapor flow due to the effect of incoming vapor. Therefore, two-phase flow and single-phase flow appeared alternatively in the microchannels, causing large fluctuations of wall temperatures as well as other measurements. It was also found that the occurrence of vapor injection flow moved from the outlet toward the inlet as the mass flux was decreased. The vapor injection flow and its induced condensation instabilities in microchannels are reported here for the first time.

Keywords: Condensation; Microchannel; Instability; Injection flow

1. Introduction

Condensation in minichannels has important applications in various compact heat exchangers. Most of the analyses on condensation heat transfer in minichannels are based on the annular flow model. Begg et al. [1] developed a physical and mathematical model of annular film condensation to predict the shape of the liquid–vapor interface along a miniature tube leading to the complete condensation phenomena in small diameter tubes. Using the annular model consisting of three zones, Zhao and Liao [2] analyzed film condensation heat transfer inside vertical mini triangular channels. Their analyses showed that the condensation heat transfer coefficient in a triangular tube is much higher than that of a round tube. Baird et al. [3] used a simple shear-driven annular flow model to predict the

* Corresponding author. Tel./fax: +86 21 6293 3107.
E-mail addresses: whysrj@sjtu.edu.cn (H.Y. Wu), pingcheng@sjtu.edu.cn (P. Cheng).

0017-9310/$ - see front matter © 2005 Elsevier Ltd. All rights reserved.
doi:10.1016/j.ijheatmasstransfer.2004.12.034

condensation heat transfer coefficient, and found that this model agreed better with their experimental data than other models.

Recent experimental work [4,5], however, show that the annular flow is not the only condensation flow pattern in minichannels. In round and rectangular tubes with hydraulic diameters in the range of 1–5 mm and mass flux of 150–750 kg/m^2 s, Garimella [4] reported four major condensation flow patterns: the annular, intermittent flow, wavy flow and dispersed flow. The intermittent regime became larger as the tube diameter was decreased. Recently, Mederic et al. [5] performed an experiment on flow condensation in circular tubes having inside diameters of 560 μm and 1100 μm respectively. They observed that slug and bubbly flows, in addition to the annular and annular-wavy flows, existed in these minitubes. They also mentioned that interfacial instabilities existed in their experiment although no measurements of such instabilities were given.

Other experimental data [6,7] suggested that the condensation phenomena in minichannels may be different from those in macrochannels. Wang et al. [6] found that existing correlations over-predicted the heat transfer in a horizontal rectangular multi-port aluminum condenser tube of 1.46 mm hydraulic diameter. Kim et al. [7] carried out an experimental investigation of R134a condensing inside a single round tube with an inner diameter of 0.691 mm. They found that the existing heat transfer correlations failed to predict their data, and the discrepancies became more obvious especially at low mass flux.

Very few experimental work has been carried out for condensation heat transfer in tubes and channels having a hydraulic diameter less than 100 μm, which have important applications to MEMS devices, micro heat pipes and micro fuel cells. The only published paper on condensation in microchannels is given by Chen and Cheng [8], who reported their preliminary experimental results on condensation of steam in silicon microchannels having a hydraulic diameter of 75 μm with a length of 80 mm. They observed intermittent flow patterns existed in these microchannels, which confirmed the findings of Garimella [4] that the intermittent regime became larger as the tube diameter is decreased.

In this paper, we have carried out further visualization and measurement experiments on condensation flow of steam in silicon microchannels under different inlet pressures from 4.15×10^5 Pa to 1.25×10^5 Pa (with corresponding mass fluxes decreasing from 47.5 g/cm^2 s to 19.3 g/cm^2 s), and with outlet at the atmospheric pressure. It is found that condensation flow patterns in microchannels depend not only on the inlet pressure and mass flux, but also on the time and location in microchannels. Of particular interest is the observation of some new periodically alternating condensation flow patterns at low mass flux in these microchannels. These alternating condensation flow patterns are akin to the alternating boiling flow patterns in microchannels, which also occur at low mass flux [9–11].

2. Experimental setup

Fig. 1 shows the experimental setup, which consisted of a water tank, a water pump, an electric boiler, a discharge valve, a steam valve, a filter, a test section, and a condensate collecting container. The deionized water in the water tank was pumped into the electric boiler, where the water was vaporized at a pressure of 5×10^5 Pa. The saturated steam from the boiler flowed successively through the valve, filter, test section, and was finally collected by a container with a hole vented to the atmosphere. Fig. 2 shows the test section, consisting of 10 parallel silicon microchannels, was cooled by a circulation of cooling water of 8 °C from the bottom of the wafer. The microchannels, having a trapezoidal cross section with a top width of 251.5 μm, bottom width of 155.7 μm, depth of 56.5 μm (with a hydraulic diameter of 82.8 μm), and length of 30 mm, were fabricated on a $\langle100\rangle$ silicon wafer (having a thickness of 0.525 mm) using the photolithography method. These microchannels were then covered with a thin transparent pyrex glass from the top. For the visualization of flow patterns in the microchannels, a high-speed video recording system connecting with a microscope, was located above the microchannels. To investigate the effect of condensation flow patterns on wall temperatures, five T-type thermocouples with a diameter of 0.1 mm and a response time of 0.1 s were embedded in the wafer directly below the middle microchannel. Also, at the inlet and outlet of the microchannels, two T-type thermocouples with a diameter of 0.1 mm and a response time of 0.1 s as well as two pressure transducers with a response time of 0.2 s were installed to measure the fluid inlet/outlet temperatures and pressures.

3. Experimental procedures

Before the experiment, the steam from the boiler was discharged by a discharge valve, thereby, evacuating the uncondensable gas in the steam. The experiment was performed by regulating different inlet pressures while keeping the outlet pressure at the atmospheric pressure (10^5 Pa). When the inlet pressure was decreased from the value of 4.15×10^5 Pa to 1.25×10^5 Pa with corresponding mass fluxes decreasing from 47.5 g/cm^2 s to 19.3 g/cm^2 s, different condensation flow patterns as well as different temperature and pressure variations were observed. These experimental results will be discussed in the next section.

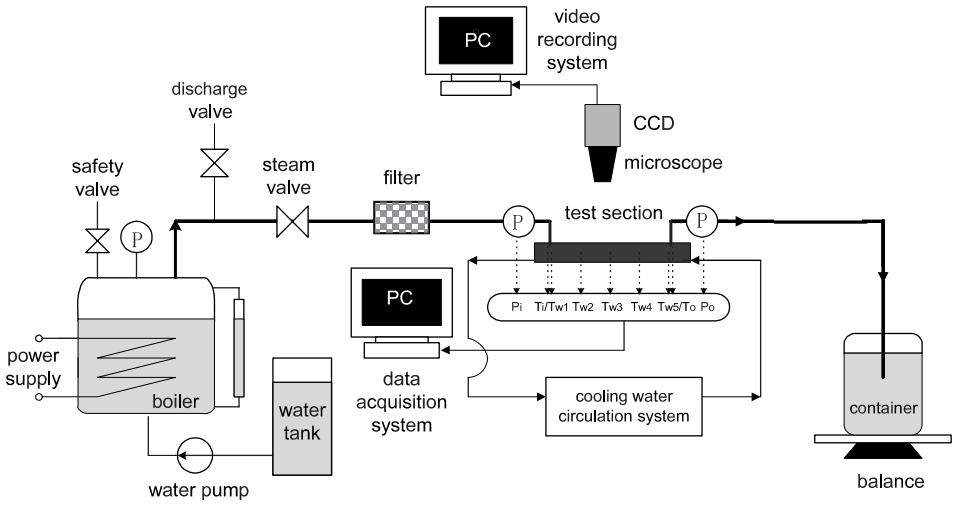

Fig. 1. Experimental system.

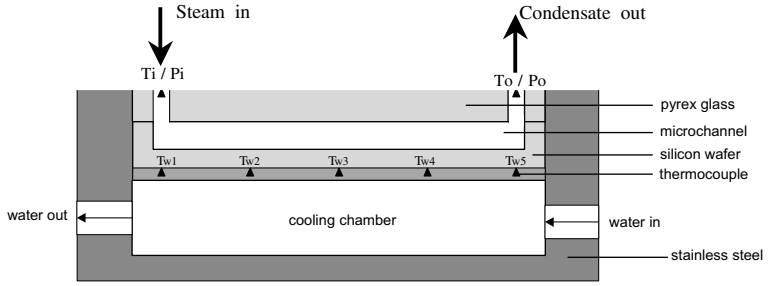

Fig. 2. Test section.

4. Results and discussion

4.1. Case I: fully droplet flow

When the inlet pressure was 4.15×10^5 Pa and the corresponding mass flux was 47.5 g/cm^2 s, droplet flow existed everywhere on the wall of the microchannels, which is sketched in Fig. 3a. Note that the flow direction in this figure was from right to left. We call this flow pattern as the "fully droplet flow". With the aids of a microscope and a high-speed video system, it was observed that water droplets were formed everywhere on the surface of the microchannel. The condensation droplets near the inlet were smaller than those near the outlet because of the gradual aggregation and coalescence of droplets along the microchannels. Figs. 3b and c show the temporal variations of temperature and pressure of the fluid at the inlet and the outlet. From these two graphs, it was found that the steam at the inlet was at saturated condition and was slightly subcooled at the outlet. However, the temporal variations of inlet and outlet temperatures and pressures were small.

Fig. 3d gives wall temperature measurements at the bottom of the silicon wafer at five different longitudinal locations at $x/L = 0, 0.25, 0.5, 0.75$, and 1 (where $x/L = 0$ and 1 represent the inlet and outlet location respectively). It was found that the temperature at the silicon wafer decreased from nearly 120 °C at the inlet to 87 °C at the outlet with the largest temperature drop between $x/L = 0.75$ to $x/L = 1$ due to the aggregation of droplets at the outlet ($x/L = 1$) as well as the side heat loss in the silicon wafer. It was also found that the temporal variations of wall temperatures for this case were small. Therefore, the fully droplet flow in the microchannels can be regarded as a steady condensation flow.

4.2. Case IIA: droplet/annular/injection/slug-bubbly flow

As the inlet pressure was decreased to 2.15×10^5 Pa and the corresponding mass flux was decreased to

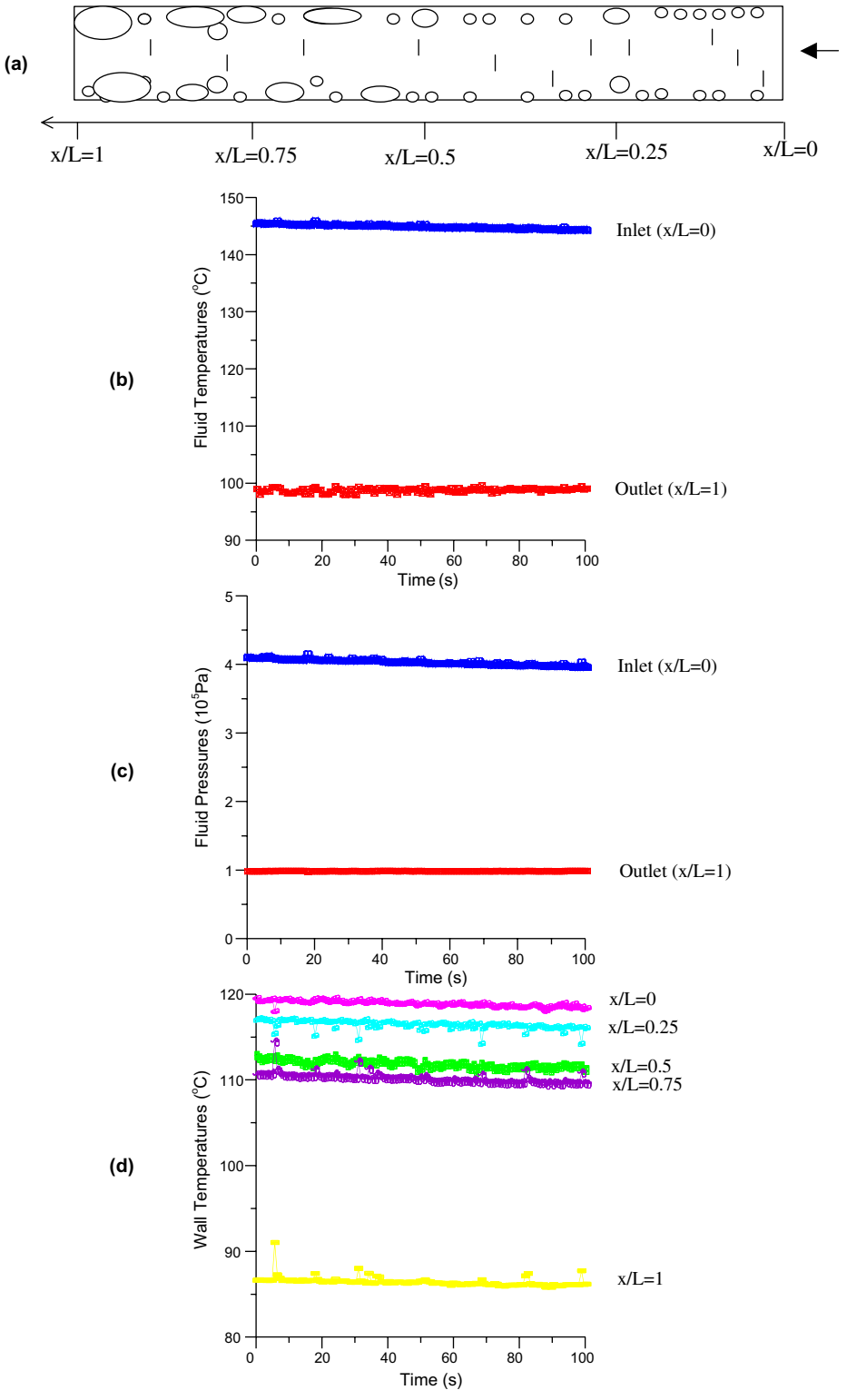

Fig. 3. Visualization and measurement results for Case I.

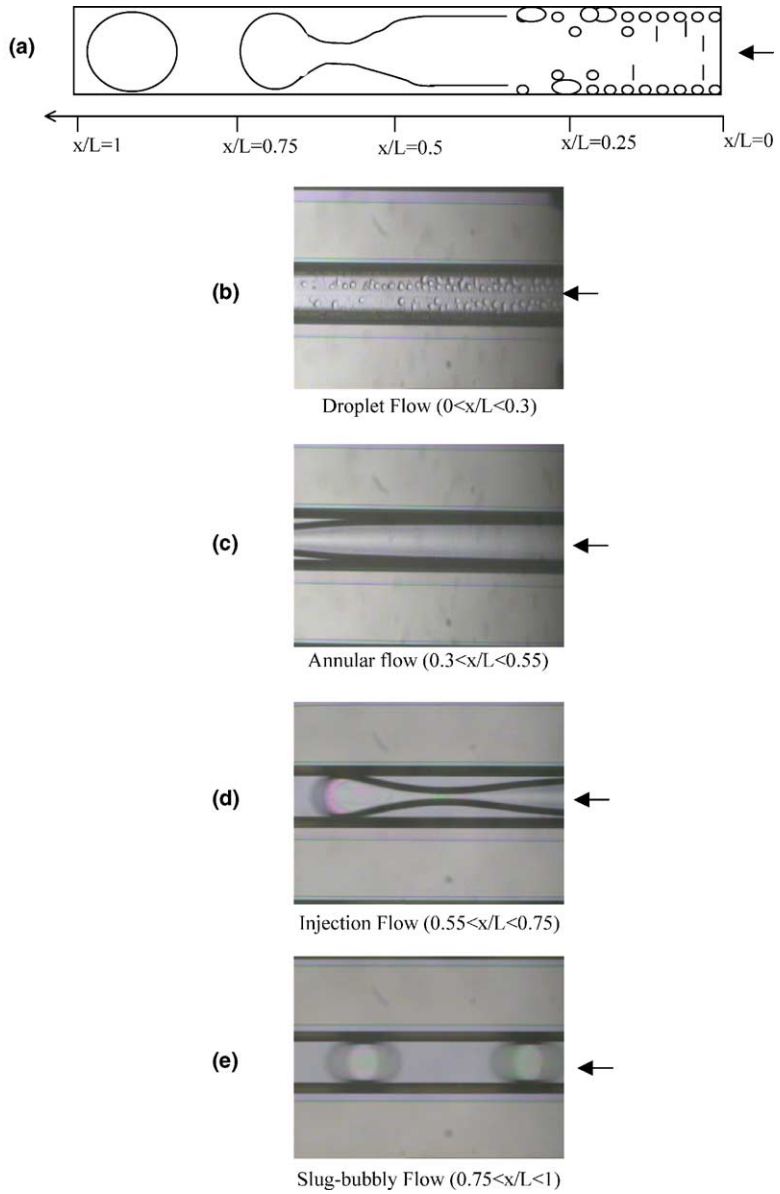

Fig. 4. Sketch and photos of four typical flow zones at different locations for Case IIA.

30.4 g/cm^2 s, a vapor injection flow, consisting of a series of bubble growth and detachment activities, occurred in the microchannels. Fig. 4a is a sketch of this flow pattern in the microchannel, where the upstream of the injection flow was occupied by the droplet flow and annular flow successively, and the downstream was occupied by the slug-bubbly flow. Figs. 4b–e give typical photos of the droplet flow ($0 < x/L < 0.3$), annular flow ($0.3 < x/L < 0.55$), injection flow ($0.55 < x/L < 0.75$), and slug-bubbly flow ($0.75 < x/L < 1$) that appeared in different zones of the microchannel at certain instant of time. From the visualization study, it could be seen that the slug-bubbly flow near the outlet was actually the detached product of the vapor injection flow. It was also found that the injection flow disappeared periodically, inducing the periodic disappearance of slug-bubbly flow at downstream and the periodic disappearance of droplet/annular flow at upstream.

Figs. 5a and b show the temporal variations of temperature and pressure measurements at inlet and outlet of the microchannels for Case IIA, where the injection flow occurred downstream of the microchannel. From these measurements, it is known that the steam at the inlet was at saturated condition and the condensate at

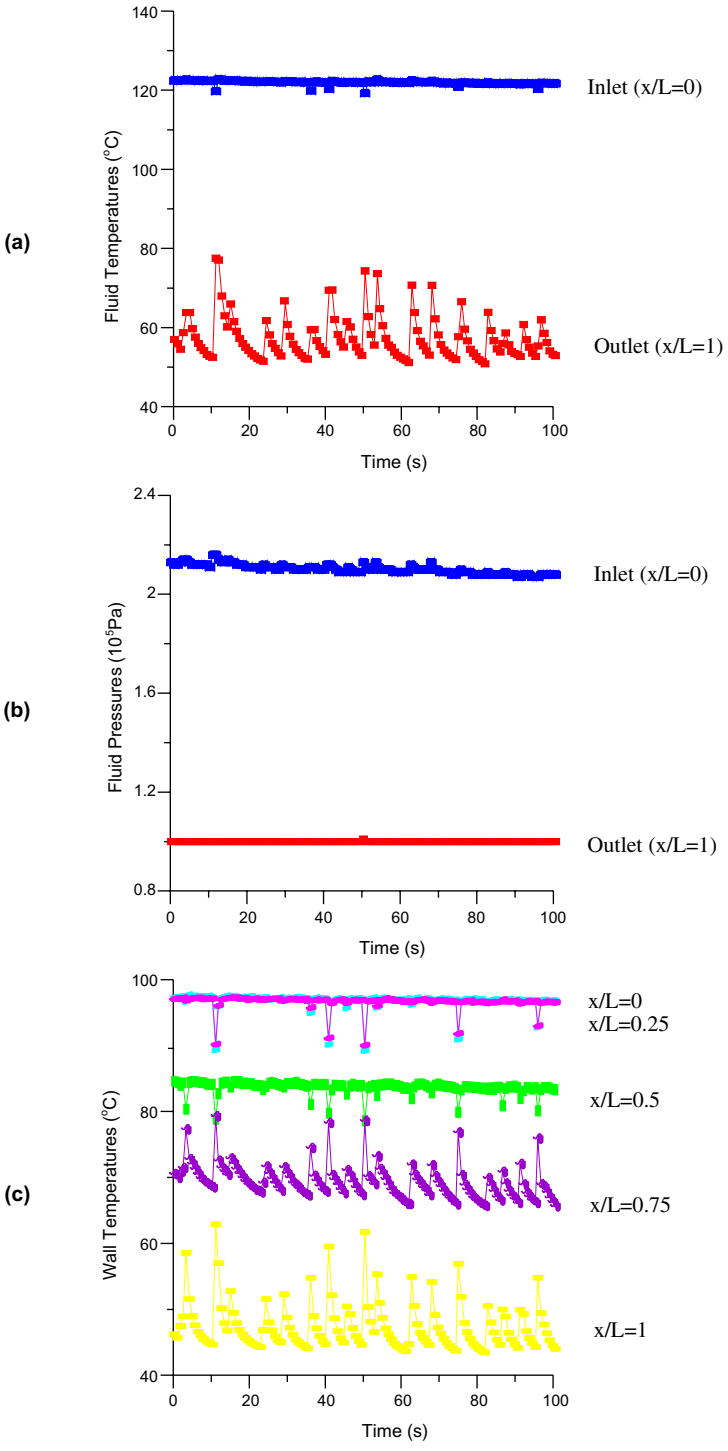

Fig. 5. Measurement results for Case IIA.

the outlet had a subcooling of 25–50 °C. It was also found that both the inlet temperature and pressure measurements had little variations with respect to time, which shows that the inlet fluid had not been affected by the periodic injection flow at downstream ($0.55 < x/L < 0.75$) and its induced condensation instability.

However, because the periodic slug-bubbly flow existed near the outlet, the outlet water temperature showed periodic fluctuations with time. Note that the outlet pressure still remained unchanged at 10^5 Pa since the outlet of the microchannels was vented to the atmosphere.

Fig. 5c shows the wall temperature decreased from 98 °C at the inlet to a time-average value of 48 °C at the outlet. It can be seen that the wall temperatures variations at the regions $x/L < 0.55$ and $x/L \geqslant 0.75$ are out of phase with each other. In particular, whenever there was a temperature decrease at $x/L < 0.55$, there was a temperature increase at $x/L \geqslant 0.75$. The wall temperatures being out of phase confirm that an injection flow occurred between these two regions because different alternation flow patterns existed at these regions. As soon as the injection flow disappeared near the middle of the microchannel, the flow alternated from droplet/annular flow to vapor flow at upstream of the injection flow ($x/L \leqslant 0.55$) while the flow alternated from slug-bubbly flow to liquid flow at downstream of the injection flow ($x/L \geqslant 0.75$). It can be seen that wall temperatures in the upstream droplet zone ($0 < x/L < 0.3$) showed small variance with time. However, wall temperatures in the slug-bubbly flow in downstream ($0.75 < x/L < 1$) show large fluctuations with time, with the maximum fluctuation amplitude of about 20 °C. These large fluctuations are owing to the reversed condensate flow after the disappearance of the injection flow. The average periods of these temperature fluctuations were about 7 s, which is consistent with the visualization result for the periodic injection flow in the microchannel.

4.3. Case IIB: annular/injection/slug-bubbly flow

When the inlet pressure was further decreased to 1.45×10^5 Pa and the corresponding mass flux was decreased to 23.6 g/cm^2 s, the visualization study showed that the injection flow occurred earlier at upstream ($0.25 < x/L < 0.5$). Because the injection flow occurred further upstream, the length of the droplet zone near the inlet was reduced, and upstream of the injection flow was found to be almost occupied by the annular flow, while downstream was still occupied by a slug-bubbly flow. Fig. 6a is a sketch of the flow pattern in the microchannel for this case, where the annular flow ($0 < x/L < 0.25$), injection flow ($0.25 < x/L < 0.5$) and slug-bubbly flow ($0.5 < x/L < 1$) occupied in different parts of the microchannel. Similar to Case IIA, the injection flow appeared periodically also. Since the disappearance period of the injection flow was prolonged in this case (about 6 s) versus about 3 s in Case IIA, the periodic phenomena of injection flow in Case IIB was more obvious than in Case IIA.

Fig. 6b gives an episode of a series of successive photos on flow patterns (in $0.25 < x/L < 0.5$) that were taken at an interval of 0.04 s for Case IIB where the periodic appearance of vapor injection flow in the microchannel can be seen. After a series of bubble growth and detachment activities ending at $t = 5.16$ s, the vapor injection flow suddenly disappeared, and a reversed condensate

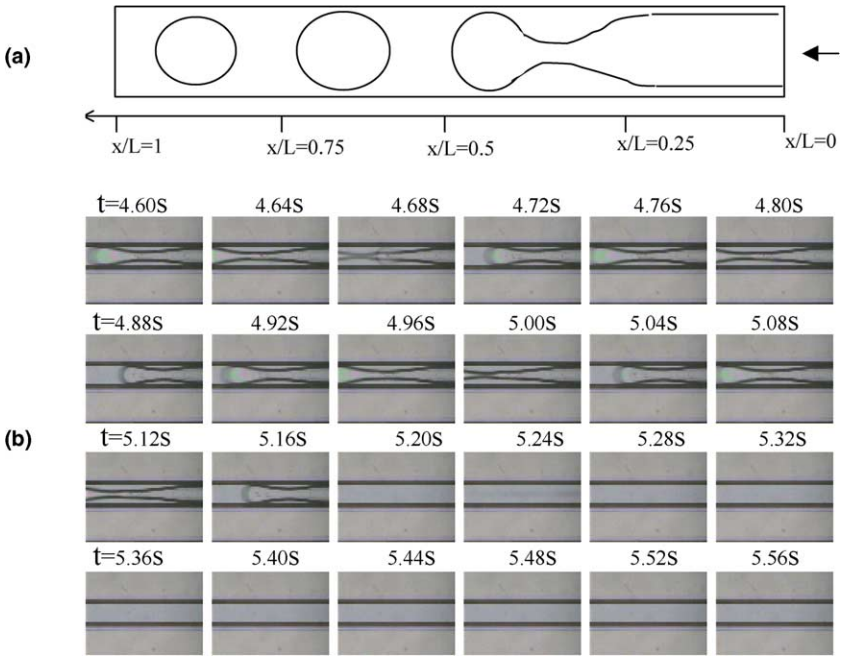

Fig. 6. Visualization results for Case IIB.

flow appeared due to the aggregation of condensates at the outlet as well as the pumping effect by the disappearance of the injection flow. After the reversed condensate flow lasted for several seconds, a new cycle of vapor injection flow appeared. According to the visualization study, the periods of injection flow and the single-phase flow during a cycle, were about 4 s and 6 s respectively. If experiment continued, this alternation from the vapor injection flow to single-phase liquid flow would repeat itself. At the same time, the upstream annular flow and the downstream slug-bubbly flow appeared periodically also. During the disappearance period of vapor injection flow, the condensate at the outlet reversed back to occupy the previous slug-bubbly zone, while the previous annular flow zone was filled with the vapor due to the combined effects of the incoming vapor and the reversing flow of the vapor core of previous injection flow. Therefore, at upstream of the injection flow, the flow alternated from the annular flow to the single-phase vapor flow periodically, while at downstream of the injection flow, the flow alternated from the slug-bubbly flow to the single-phase liquid flow periodically. According to the visualization study, the alternation period (consisting of appearance period and disappearance period) was about 10 s, longer than the alternation period in Case IIA (7 s).

Figs. 7a and b show the temporal variations of temperature and pressure measurements of the fluid at the inlet and outlet of microchannels for Case IIB. From these data, it can be found that the steam at the inlet was at saturated condition while the condensate at the outlet had a large degree of subcooling of 60–70 °C. Due to the occurrence of the injection flow at further upstream (at $0.25 < x/L < 0.5$), the fluctuation-amplitude of outlet temperature was smaller than that in Case IIA, while the fluctuation-amplitude of inlet temperature was larger than that in Case IIA. As shown in Fig. 7b, the outlet pressure in this case was still maintained at the atmosphere value of 10^5 Pa, while the inlet pressure showed fluctuations with time due to the occurrence of injection flow nearer the inlet.

Fig. 7c presents the temporal variations of wall temperatures for Case IIB. It is seen that all wall temperatures show large fluctuations with time. Moreover, the fluctuations of wall temperatures at the upstream of the injection flow ($x/L \leqslant 0.25$) and those at the downstream ($x/L \geqslant 0.5$) of the injection flow are at same frequency but are out of phase. A simultaneous visualization exploration shows that this out-of-phase fluctuations of wall temperatures was caused by the different alternating flow patterns at these locations, that is, at upstream of the injection flow, the flow alternated from the annular flow to single-phase vapor flow periodically, while at the downstream of injection flow, the flow alternated from the slug-bubbly flow to single-phase liquid flow periodically as discussed earlier. Affected by the alternation from the annular flow to the vapor flow, the wall temperatures at $x = 0$ and 0.25 fluctuated from the lower value of the annular flow to the higher value of the vapor flow, while affected by the alternation from the slug-bubbly flow to the single-phase liquid flow, the wall temperatures at $x = 0.5$, 0.75 and 1 fluctuated from the higher value of the slug-bubbly flow to the lower value of the single-phase liquid. Thus, the fluctuations of wall temperatures at $x = 0$ and 0.25 are in out-of-phase with the fluctuations of wall temperatures at $x = 0.5, 0.75$ and 1. From Fig. 7c, it is found that the fluctuation period of various wall temperatures was about 10 s, consistent with the visualization results.

4.4. Case III: fully slug-bubbly flow

Fig. 8a is a sketch of flow pattern for Case III, when the inlet pressure was further decreased to 1.25×10^5 Pa with the corresponding low mass flux of 19.3 g/cm^2 s. In this case, the vapor injection flow occurred at the inlet and the annular flow disappeared totally from the microchannel, while the slug-bubbly flow occupied everywhere in the microchannels. We call this flow pattern as the "fully slug-bubbly flow". Under this condition, the vapor bubble and liquid slug appeared alternatively along the microchannels, which has been referred to as the "intermittent flow" in the literature. It is noted that due to the accumulation of the condensate, the liquid slug became larger along the flow direction in the microchannels, while the vapor bubble became smaller along the microchannels. With the aids of a high-speed video system, it was also found that the slug-bubbly flow appeared periodically. As soon as the injection flow disappeared from the inlet, a reversed condensate flow appeared and the slug-bubbly flow disappeared. Therefore, the flow alternated from the intermittent slug-bubbly to single-phase liquid flow in the microchannel with an alternation period of about 20s for this case with a low mass flux.

Figs. 8b and c show the temporal variations of fluid temperatures and pressures at the inlet and outlet of the microchannels for Case III. It is shown that the inlet steam fluctuated from the saturated to subcooling periodically while the condensate at the outlet was at room temperature of 20 °C (i.e., a subcooling of 80 °C). Since the injection flow occurred at the inlet, the fluctuations in inlet temperature and pressure in this case were larger than those in previous cases while the outlet temperatures and pressure showed little variations with respect to time. A further comparison of Fig. 8b and c shows that the fluctuations of inlet temperature and inlet pressure were out of phase in this case. This out of phase fluctuation is attributed to the fact that the reversed flow of the condensate has reached the inlet, which will be explained below. When the reversed condensate flow

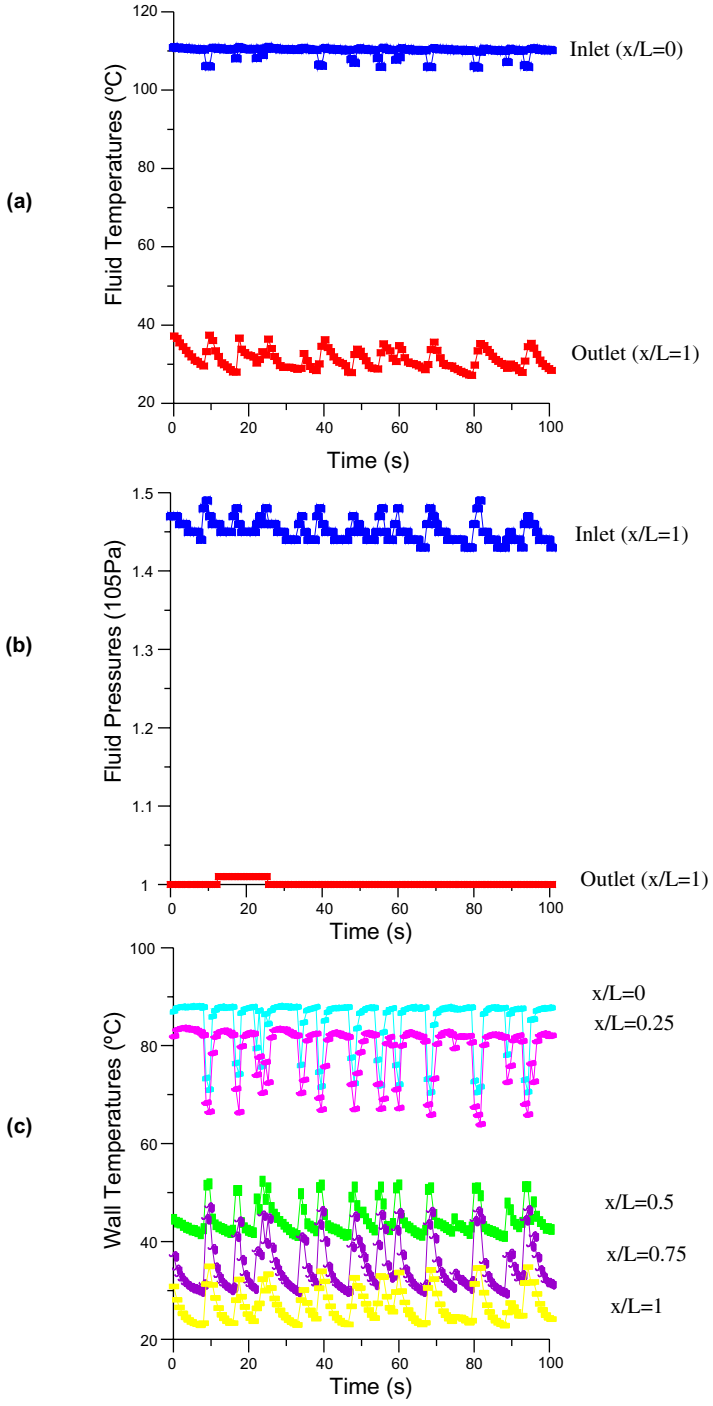

Fig. 7. Measurement results for Case IIB.

occurred, the incoming vapor at the inlet was facing a large flow resistance. Therefore, the inlet pressure rose, while the inlet steam temperature was decreased due to the effect of condensate. When the reversed condensate flow disappeared, the flow resistance decreased. Thus, the inlet pressure dropped, while the inlet temperature increased due to the reappearance of slug-bubbly in the microchannel.

Fig. 8d shows the temporal variations of wall temperatures at different locations in the microchannel where a

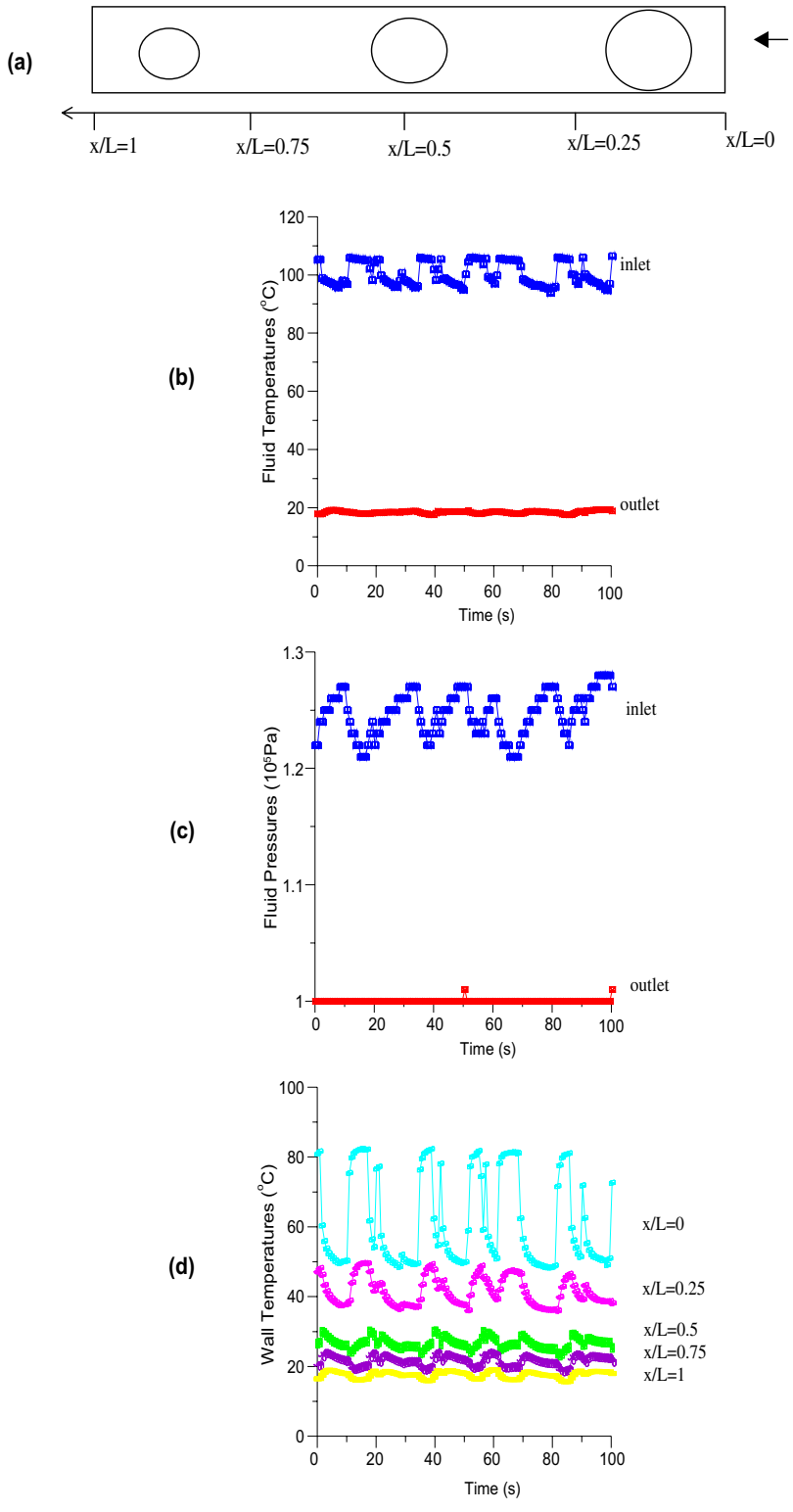

Fig. 8. Visualization and measurement results for Case III.

fully slug-bubbly flow (corresponding to the high-temperature regime) and a fully liquid flow (corresponding to the low temperature regime) appeared alternatively, causing large fluctuations of wall temperatures. It is found from this figure that although the fluctuation period and phase were the same at different locations, the fluctuation amplitudes of wall temperatures were greatly different. Since the injection flow in this case occurred at the inlet, the fluctuation amplitudes of wall temperature near the inlet were larger than those near the outlet (with the fluctuation amplitude of wall temperature corresponding to the inlet can be up to 30 °C). Also, the fact that the vapor bubble became smaller along the flow direction contributed to the decreasing fluctuation amplitudes of wall temperatures along the flow direction. According to the measurements, the fluctuation period of wall temperatures was about 20 s, longer than those in Cases IIA (7 s) and IIB (10 s).

4.5. Effect of flow nonuniformity

As mentioned earlier, 10 parallel microchannels were used in this experimental investigation. However, most of the above discussion was focused on the middle microchannel where the photos were taken from above the channel, and the wall temperatures were measured below the channel. According to our observations, flow in these microchannels was actually not exactly the same. Since the inlet and outlet ports were closer to the middle microchannel, the flow rate in the middle channel was larger than that in the other channels. Therefore, the vapor injection flow in the middle microchannel appeared further downstream than in other microchannels. Thus, the injection flow and its induced condensation instabilities occurred earlier in the side microchannels as compared with the middle microchannel.

5. Concluding remarks

In this paper, a visualization and measurement experiment has been carried out to investigate condensation flow patterns in microchannels for different inlet pressures but at the same outlet pressure. It is found that:

1. The condensation flow pattern of steam in the microchannel depends greatly on the amount of condensation mass flux. The flow pattern also depends on the location in microchannel and time.
2. With decreasing mass flux, different condensation flow patterns appeared in the microchannels: a fully droplet flow, a droplet/annular/injection/slug-bubbly flow, an annular/injection/slug-bubbly flow, and a fully slug-bubbly flow.
3. The periodic appearance of injection flow and its induced periodic appearances of droplet/annular flow at upstream and slug-bubbly flow at downstream caused fluctuations of the wall temperatures.
4. The wall temperatures near the location, where the vapor injection flow occurred, fluctuated more acutely.
5. Due to the different alternation flow patterns at upstream and downstream of the injection flow, temperature fluctuations in these two zones are out of phase.
6. The fluctuation periods of wall temperatures and other measurements increase with the decrease in mass flux.
7. The injection flow and its induced condensation instabilities appeared further upstream in the side microchannels than in the middle microchannel.
8. Condensation instability and its induced fluctuations of various measurements should be taken into consideration in microchannels having hydraulic diameters less than 100 μm at low mass flux.

Acknowledgement

This work was financially supported by the National Natural Science Foundation of China (Grant No. 50476017). The authors would like to thank Mr. Billy Chin-Pang Siu for his assistance in the fabrication of the microchannels and Dr. Yi-Kuen Lee for his helpful discussion in this project.

References

[1] E. Begg, D. Khrustalev, A. Faghri, Complete condensation of forced convection two-phase flow in a miniature tube, ASME J. Heat Transfer 121 (1999) 904–915.
[2] T.S. Zhao, Q. Liao, Theoretical analysis of film condensation heat transfer inside vertical mini triangular channels, Int. J. Heat and Mass Transfer 45 (2002) 2829–2842.
[3] J.R. Baird, D.F. Fletcher, B.S. Haynes, Local condensation heat transfer rate in fine passages, Int. J. Heat and Mass Transfer 46 (2003) 4453–4466.
[4] S. Garimella, Condensation flow mechanisms in microchannels: basis for pressure drop and heat transfer models, in: Proc. of the First International Conference on Microchannels and Minichannels, Rochester, New York, USA, April 21–23, 2003, pp.181–192.
[5] B. Mederic, M. Miscevic, V. Platel, P. Lavieille, J.L. Joly, Complete convective condensation inside small diameter horizontal tubes, in: Proc. of the First International Conference on Microchannels and Minichannels, Rochester, New York, USA, April 21–23, 2003, pp.707–712.
[6] W.W.W. Wang, T.D. Radcliff, R.N. Christensen, A condensation heat transfer correlation for millimeter-scale tubing with flow regime transition, Exp. Thermal Fluid Sci. 26 (2002) 473–485.

[7] M.H. Kim, J.S. Shin, C. Huh, T.J. Kim, K.W. Seo, A study of condensation heat transfer in a single mini-tube and a review of korean micro- and mini-channel studies, in: Proc. of the First International Conference on Microchannels and Minichannels, Rochester, New York, USA, April 21–23, 2003, pp. 47–58.
[8] Y.P. Chen, P. Cheng, Condensation of steam in silicon microchannels, Int. Commun. Heat and Mass Transfer 32 (2005).
[9] H.Y. Wu, P. Cheng, Visualization and measurements of periodic boiling in silicon microchannels, Int. J. Heat and Mass Transfer 46 (2003) 2603–2614.
[10] H.Y. Wu, P. Cheng, Liquid/two-phase/vapor alternating flow during boiling in microchannels at high heat flux, Int. Commun. Heat and Mass Transfer 30 (3) (2003) 295–302.
[11] H.Y. Wu, P. Cheng, Boiling instability in parallel silicon microchannels at different heat flux, Int. J. Heat and Mass Transfer 47 (2004) 3631–3641.